LA-UR- 10-03102

Approved for public release; distribution is unlimited.

Title:	The First Measurements of Soft X-ray Flux from Ignition Scale Hohlraums at the National Ignition Facility using DANTE
Author(s):	J. L. Kline, K. Widmann, A. Warrick, R. E. Olson, C. A. Thomas, A. S. Moore, L. J. Suter, O. Landen, D. Callahan, J. Liebman, A. Conder, S. N. Dixit, P. Torres III, V. Tran, E. L. Dewald, J. Kamperschroer, L. J. Atherton, S. Azevedo, R. Beeler Jr, J. Celeste, D. Larson, B. J. MacGowan, S. H. Glenzeb, D. Hinkel, D. Kalantar, R. Kauffman, J. Kilkenny, N. Meezan, M. D. Rosen, M. Schneider, E. A. Williams, S.
Intended for:	18th Topic Conference on High Temperature Plasma Diagnostics Idlewood, NJ May 16th-20th, 2010

Los Alamos
NATIONAL LABORATORY
EST.1943

Form 836 (7/06)

The First Measurements of Soft X-ray Flux from Ignition Scale Hohlraums at the National Ignition Facility using DANTE

J. L. Kline[a], K. Widmann[b], A. Warrick[b], R. E. Olson[e], C. A. Thomas[b], A. S. Moore[c], L. J. Suter[b], O. Landen[b], D. Callahan[b], J. Liebman[b], A. Conder[b], S. N. Dixit[b], P. Torres III[d], V. Tran[d], E. L. Dewald[b], J. Kamperschroer[b], L. J. Atherton[b], S. Azevedo[b], R. Beeler Jr.[b], L. Berzins[b], J. Celeste[b], D. Larson[b], B. J. MacGowan[b], S. H. Glenzer[b], D. Hinkel[b], D. Kalantar[b], R. Kauffman[b], J. Kilkenny[f], N. Meezan[b], M. D. Rosen[b], M. Schneider[b], E. A. Williams[b], S. Vernon[b], R. J. Wallace[b], B. Van Wonterghem[b], & B. K. Young[b]

[a]*Los Alamos National Laboratory, Los Alamos, New Mexico, 87545, USA*
[b]*Lawrence Livermore National Laboratory, Livermore, CA 94550, USA*
[c] *Atomic Weapons Experiments, Aldermaston, RG74PR, UK*
[d] *National Security Technologies, Livermore Operations, Livermore, CA 94550, USA*
[e] *Sandia National Laboratory, Albuquerque, NM, 87185, USA*
[f] *General Atomics, San Diego, CA, 92121, USA*

The first 96 and 192 beam vacuum hohlraum have been fielded at the National Ignition Facility demonstrating radiation temperatures up to 340 eV and fluxes of 20 TW/sr representing a 20 times flux increase over NOVA/Omega scale hohlraums. The vacuum hohlraums were irradiated with 2 ns square pulses with energies between 150 – 635 kJ. They produced nearly Planckian spectra with about 30±10% more flux than predicted by the current radiation hydrodynamic simulations after careful verification of all component calibrations (which included an ≈ 10% downward correction to Center X-Ray Optics opacities just below the Cu L edge at 50-750 eV), cable deconvolution, and analysis software routines. To corroborate these results, first a half hohlraum experiment was conducted using a single 2 ns-long axial quad with an irradiance of ~1-2 x 10^{15} W/cm^2 for comparison with NIF Early Light experiments completed in 2004. Second, we completed a conversion efficiency test using a 128-beam nearly uniformly illuminated gold sphere with intensities kept low (at 1 x 10^{14} W/cm^2 over 5 ns) to avoid sensitivity to modeling uncertainties for non-local heat conduction and non-linear absorption mechanisms, to compare with similar intensity, 3 ns OMEGA sphere results. The 2004 and 2009 NIF half-hohlraums agreed to 10% in flux, but more importantly, the 2006 OMEGA Au Sphere, the 2009 NIF Au sphere and the calculated Au conversion efficiency agree to ±5% in flux, which is estimated to be the absolute calibration accuracy of the DANTEs. Hence we concluded the 30±10% higher than expected radiation fluxes from the 96 and 192 beam vacuum hohlraums are attributable to differences in physics when we transitioned to large hot hohlraums. Specifically, using variants in the atomic physics models and electron heat conduction, newer simulations show that nonlocalization of energy deposition leads to less energy being stored in the coronal plasma leading to higher x-ray conversion efficiency. Since the larger volume-to-area ratio hohlraums have large coronal plasmas which scale volumetrically, the reduction in energy losses to the corona become more pronounced than for smaller NOVA/Omega scale hohlraums. The higher conversion efficiencies are also consistent with observations from other 1 ns gold sphere experiments conducted at Omega with 1 x 10^{15} W/cm^2 laser irradiances.

I. Introduction

Hohlraums are often used in high energy density laboratory plasma experiments to convert the laser energy to a near Planckian soft x-ray spectrum. The generated radiation flux provides the ablative pressure drive for investigating a number of different area of physics such as: capsule implosions, hydrodynamic instabilities,[1,2] equation of state experiments,[3] astrophysics,[4] and radiation transport.[5] Thus, it is vital to measure the time dependent soft x-ray flux in order to characterize these experiments, and at the National Ignition Facility the flux is measured using the Dante[6,7] diagnostic. Dante is an 18 channel soft x-ray spectrometer that uses a series of K- and L- edge filters, mirrors, and x-ray diodes (XRD) to determine the absolutely calibrated flux in a series of energy bands between 50 eV and 20 keV. A spectral unfold algorithm then uses the measured signals in each band to back out an emission spectrum from which the total drive flux is determine by integrating the spectrum. This is done for each recorded time to provide the temporal evolution of the flux.

Prior to ignition experiments at the NIF in 2009,[8-10] the experimental diagnostics required re-activation since the were not used since the NIF early light experiments.[11-15] As part of this process, a series of scale-0.7 hohlraum experiments with increasing laser energies were conducted to inaugurate multi-bundle high energy operations on the NIF, as well as test the experimental diagnostics including Dante. During these experiments, the scale-0.7 hohlraums produced about 30%±10% more flux than expected based on radiation hydrodynamic simulations benchmarked against Nova and Omega Dante measurements. These surprising results prompted an effort to carefully scrutinize Dante's operation which consisted of:

1- Review of hardware calibrations and software analysis tools.

2- A conversion efficiency test using a 128-beam nearly uniformly illuminated gold sphere with intensities sufficiently low (at 1 x 10^{14} W/cm^2 over 5 ns) to avoid sensitivity to modeling uncertainties for non-local heat conduction and non-linear absorption mechanisms to compare with earlier similar intensity 3 ns OMEGA sphere results.[16]

3- A half hohlraum experiment using a single 2 ns-long axial quad with an irradiance of ~1-2 x 10^{15} W/cm^2 for comparison with a nearly identical NIF Early Light (NEL) experiments completed in 2004.[15,17]

The results of this effort have found the Dante is working within the nominal operating parameters. With this work, the focus of the higher flux has turned towards understanding the physics that explains the additional flux. In this manuscript, details of the performance of Dante are presented based on tests used to verify proper operation of the diagnostic, including highlights of the calibration review, results of the conversion efficiency, and tests comparison with experimental results obtained during the NIF early light.

II. Flux measurements from scale-0.7 vacuum hohlraums

Vacuum hohlraum 70% of the size of full ignition scale, scale-0.7, were used for the first set of experiment initiating multi-bundle full scale operation of the National Ignition Facility. The vacuum hohlraums were 6.4 mm long, 3.55 mm in diameter with a Laser Entrance Hole (LEH) size of 2.65 mm in diameter (Figure 1). The experiments used both a 96- and a 192-beam configuration with energies ranging from 150 – 635 kJ at 351 nm in 2 ns square pulses. For the 96-beam configuration, only the beams at 30° and 50° were used. The beams were smoothed using polarization smoothing, 45 GHz Smoothing by Spectral Dispersion (SSD), and Continuum Phase Plates (CPPs). The total laser energy and power delivered by each quad is measured with ±2% and ±3% accuracy, respectively. The soft x-ray flux is measured by Dante at 37° with respect to the hohlraum axis.

Measurements of the peak soft x-ray flux from the scale-0.7 hohlraums is shown in Figure 2. The data show the flux during these experiments reached values close to 20 TW/sr. The associated temperatures are also plotted in Figure 2 that reached values of ~340 eV. Such temperature were only possible on previous laser facilities with volumes 50 times smaller. The dashed curve represents the initial pre-shot calculations for the experiments form LASNEX using the standard ignition configuration. This includes a XSN line averaged atomic physics model and flux limited heat diffusion model with a flux limit of 0.05. The results shows that the measured flux is 20-30% higher than predicted. The data can be explained using a Detailed Configuration Atomic Physics model that includes two electron processes and a flux limit of 0.15 shown as the solid curve in Figure 2. Since modeling of the experiments can produce a wide range in terms of the flux produced by these hohlraums, it is vital to validate Dante's operation so that an understanding of the physics is possible by validating one of the models.

II. Scrutinizing Dante hardware and software

As part of the operational verification of the Dante, every aspect of the instrument's performance has been examined. The Dante team examined the calibrations of all components, as well as the analysis software. During this undertaking, four key aspects of the Dante operations became the focal points, compensation for cable dispersion between the XRDs and the recording oscilloscopes, the unfold algorithm, the sieves, and calibration of a couple of the edge filters. Details of the scrutinization for the first three elements are given in this section. Details of calibration of the components and associated errors can be found in presentation by Widmann *et al.* in these proceedings.

IIa Cable Compensation

Because of the expected high neutron fluxes generated during thermonuclear ignition experiments, the diagnostics mezzanines that house the recording oscilloscope for the diagnostics is located behind a 10 ft think shielding wall leading to long cable runs between detectors and recorders. Using such long lengths of cables introduces signal dispersion as well as attenuation which must be compensated. For Dante, the cable system used to connect the XRDs to the oscilloscope comes in three sections. On both ends there is a jumper cable that connects the oscilloscope on one end and the XRDs on the other end to the main signal cable through a junction box. The cables are made from Times Microwave LMR-300 with the two section approximately xx and xx in length. The main cable run is a ~165 ft of Times Microwave LMR-600. Since the attenuation, as well as the dispersion is frequency dependent, calibration of the cables is required to deconvolve the measured signal and retain the original signal generated by the XRDs.

The cables are calibrated using a signal generator attached to one end of the cable system and recording the applied 10 ns square pulse. Using the input, x(t), and output, y(t), signals for the cable the transfer function, H(t), can be computed in Fourier space, i.e. y(t) = H(t)x(t) => y(f) = H(f)x(f) to determine the frequency dependent cable response $H^{-1}(f)$= y(f)/x(f). With the determination of the transfer function, the measured signals can be compensated for effects of the cabling. While the cable compensation can be done in either the time or frequency domain, The frequency domain has the advantage of For the Dante signals on the NIF, a constrained least square filter is used for the deconvolution:

$$H(f)^{-1} = \frac{X(f)conj(y(f))}{(Y(f)2+G)}. \quad (1)$$

Here, G is equal to a coefficient times the ratio of xxx. shows an example of the input and output of the square pulse used to calibrate the cables. The deconvolution of the output signal is also

shown that was done used the filter constructed by the measurement. An example of the deconvolution of an ignition pulse shape applied to the cable is shown in Figure 3b. The input and output signals are plotted in conjunction with the signal obtained using the deconvolution algorithm. The test demonstrates the ability of the algorithm to accurately reconstruct the input signal for ignition pulse shapes. In addition to the ignition pulse shapes and number of other pulses were successfully tested included a series of incremented steps which as a test should satisfy most requested pulse shapes.

IIb Sieves

The energy available on the NIF makes it possible to heat ignition scale hohlraum targets to radiation temperatures that produce soft x-ray fluxes more than an order of magnitude greater than Nova/Omega targets. Since the XRDs are limited by the Child-Langmuir law, the x-ray flux impinging on the XRD surface must be reduced. This cannot be done either by limiting the XRD aperture or adding more filtering. In the case of adding more filter, the signal passing through in either the K- or L- edges will be reduced at a greater rate than the attenuation at higher energies. This allows photons in the Au m-band region to contaminate the channels in the black body region not used in conjunction with a mirrored, i.e. channels 5-9 (.7-1.4 keV). While the a series of high energy channels are used to compensation the lower energy channels, minimizing this effect reduces the error in the measurements. [7] A reduction in the aperture size at the XRD, thus reducing the collection solid angle, will not work either. The Child-Langmuir limit for the XRD scales proportionately with the area since the limit depends on the current density between the anode and cathode. One solution is to add a pinhole array, i.e. a sieve, to the filter pack.[18] Using such a pinhole array reduces the amount of flux per unit area that hits the XRD.

The sieves designed for ignition scale targets are a 50 x 50 pinhole array machined on a 25 micron thick Tantalum substrate. The holes are tapered having a 50 micron diameter on the front side and a 62 micron diameter on the backs side with a center-to-center spacing of 150 microns. The pinhole area is mounted with the filter pack setting 1 m from target chamber center and x cm from the XRDs. This results in a magnification of each pinhole image on the XRD of 1/7 making objects ~ 3mm in diameter ~ 500 microns that leads to about 8 images overlapping at any location on the XRD. The designed transmission can be calculated for the hole diameter and spacing and gives a transmission of $T \sim \pi(25/150)^2 = 0.087$ or 8.7%. However, this assumes no variations in the hole sizes or spacing across grid which turns out not to be the case. Thus, each sieve requires its own calibration.

A sealed light box is used to calibrate the sieve transmission (Figure 4). The light box uses a Luxeon V Light Source and Hammamatsu S3584-08 silicon detector. A wall in the light box separates the light source and the detector regions with a place to mount the sieves. The distance between the light source and the sieve mounted to the wall is xx cm and from the wall to the detector is xx cm. The sieves are mounted in the same orientation as used in Dante with small end of the tapers facing the light. Measurements are made with and with the sieve to determine the transmission of the sieves.

Figure 3: **a) input and output from a cable calibration from which the least squares filter is derived with (○) is every 50 point from the cable input, (– – –) is the output, and (—) is the result using filter to deconvolve the measured cable response for the input. The plot also shows the input signal recovery from application of the filter. b) an example of an in situ calibration of a cable using an ignition pulse shape.**

Figure 4 shows the calibration of the five sieves used for the lower Dante. The calibrations have been compared with contact radiographs as well as a in situ calibration in which two channels used the same filter material but one with and the other without a sieve. Each of these values is consistent with the light box calibrations.

IIc software

The analysis algorithm for Dante is a descendent of that brought to the ICF program by Kornblum *et al.*[7] For use on the NIF as part of the shot analysis and data visualization, the routines were formally re-written with some minor modifications described in this section. The algorithm uses a rudimentary fit to the first nine channels, those with edges below 2 keV, to set a black body spectrum with the best radiation temperature. It fits these channels by comparing the measured channel voltage with a calculated voltage using the spectrum convolved with the channel response function, i.e.

$$V_i \sim \int R_i(h\nu) S(h\nu) d(h\nu) d\Omega_i$$

where V_i is the i^{th} calculated channel voltage, $R_i(h\nu)$ is the i^{th} channel response function, $S(h\nu)$ is the emission spectrum, and $d\Omega_i$ is the i^{th} channel's solid angle. Once the initial black body spectrum is determined, a broad band Gaussian bump is added to the spectrum to represent the Au -band region using channel 11, a broadband channel set to measure the flux in this region of the spectrum. At this point, the algorithm starts at the highest energy channel and adds or subtracts flux based on the difference between the measured and calculated voltages using a Gaussian representing the channel. This is done for a fixed number of iterations set by a convergence study. Typically, the spectrum has converged to within ~ 1% in 4-5 iterations, but typically 10 iterations are used. In past versions of this algorithm, the centroid of the Gaussian functions representing each channel were set by finding the point at which the calculated voltage

reached half the total voltage. The parameters for the Gaussian functions were also set manually including the centroids. The algorithm has now been modified to set the centroid and widths of the Gaussian functions based on the k- and l- edge regions of the each channels response function.

Verification of the modified algorithm was done by comparisons of a test set of data analyzed with the original routine and the production version used to analyze current data from the NIF. In addition to these comparison, both the NIF early light data and the half hohlraum experiment from 2009 were analyzed using multiple versions of the unfold algorithm that have been used to analyze Dante from recent Omega campaigns and NIF early light including the algorithm used by Sandia National Lab. In addition, a new algorithm which uses a matrix approach was also applied to the data. This work examined variation due to the selection of the Gaussian parameters and the number of iterations. The tests showed all of the results were consistent to within less than 1%.

III. Conversion Efficiency using Spherical Target

To ensure there was not a gross miscalibration of Dante, an experiment shooting a gold sphere to measure the conversion efficiency was conducted.[16] If the higher fluxes measured from the hohlraum reached values greater than 100%, there would be a clear indication of an error in the operation of Dante. In addition, the results are also be compared with previous experiments that measured the conversion efficiency from gold spheres of the same size and similar laser intensities.[16]

The target used for this experiment was a 2.1 mm plastic sphere covered with XX microns of Au. The sphere was illuminated with 112 beams and a total of 70 kJs in a 5 ns pulse

(Figure 5). The irradiance of the beams was ~1 x10^{14} W/cm^2 as in recent experiments at the Omega laser.[16] Figure 6a shows the laser pulse shape compared with the radiation flux as measured by Dante. The plot clearly shows that the radiated power is less than the total laser energy indicating the fact that there is not a major error in Dante's operation. Integrating the total laser power and radiated soft x-ray power gives a total conversion efficiency at 6.5 ns is 88.5%. This is consistent with the experiments at the Omega laser in which the conversion efficiency reached . Figure 6b shows the data compared with simulations using LASNEX.[19] The simulations are in good agreement with the experiments where the simulations have a conversion efficiency of 90% at 6 ns.

IV. Half Hohlraum Experiment

Another test of Dante's performance was a comparison with experiments conducted during NIF early light using half hohlraums.[15] The experiment used NOVA scale-1 half hohlraum 1.5 mm long, 1.6 mm in diameter, and a laser entrance hole diameter of 1.2 mm as in the NEL experiments (Figure 7). The half hohlraum was aligned along beam line 31B with the laser focused at the laser entrance hole. The experiments used a 2 ns square laser pulse with 12.25 kJ of energy. This was slightly lower than the NIF early light experiments which had 13.1 kJ in the same pulse shape. The intensity between two experiments was also slightly different since the current experiments used a scale-1 CPP having an elliptical spot with a major radius of 0.82 cm and a minor radius of 0.59 cm. This gives an irradiance of 4 x 10^{14} W/cm^2. The NIF early light experiments used a scale-0.7 CPP having a major radius of 0.42 cm and a minor radius of 0.24 and an irradiance of 2 x 10^{15} W/cm^2. The different spot sizes also lead to a small difference in the region of the back wall illuminated by the laser as view by Dante.

Figure 8 shows a comparison between the measured x-ray flux from the current experiments and those measured during NIF early light. The flux between the two shots is comparable. Since the laser energy is about 6.5% lower in the current half hohlraum experiments, the current experiments have a 6.5% larger flux than in the NEL experiments. Taking into account the larger spot size due to the larger phase plate, this measurement is within the error of Dante. Thus, the results are consistent showing that there is no major difference in Dante's operation over the past six year.

V. Conclusions

An extensive effort has gone into verifying the operational performance of Dante on NIF. This has been done through a complete review of both the component calibrations and the calibration process, including an emphasis on compensation for the signal cables. The analysis software has also undergone an extensive review including modifications to the algorithm needed for the real time data analysis. As a validation of this work, two experiments have been conducted, a conversion efficiency test using a gold sphere target and a half hohlraum target. Both experiments shows that Dante is working with its nominal operating errors. These results support the fact that the measured fluxes in the NIF scale-0.7 are higher than the initial predictions by 20-30%.

Acknowledgements

We wish to thank the NIF operations team for which these experiments would not have been possible. This work performed under the auspices of the U.S. Department of Energy by

LANL under contract DE-AC52-06NA25396, by LLNL under Contract DE-AC5 2-07NA27344, and by SNL under contract DE-AC04-94AL85000.

References

[1] D. K. Bradley, S. T. Prisbrey, R. H. Page et al., Physics of Plasmas **16** (4), 042703 (2009).
[2] J. A. Cobble, T. E. Tierney, N. M. Hoffman et al., Physics of Plasmas **13** (5), 056304 (2006).
[3] B. Remington, G. Bazan, J. Belak et al., Metallurgical and Materials Transactions A **35** (9), 2587 (2004).
[4] P. Rosen, J. Foster, B. Wilde et al., Astrophysics and Space Science **322** (1), 101 (2009).
[5] C. A. Back, J. D. Bauer, O. L. Landen et al., Physical Review Letters **84** (2), 274 (2000).
[6] E. L. Dewald, K. M. Campbell, R. E. Turner et al., Review of Scientific Instruments **75** (2004).
[7] H. N. Kornblum, R. L. Kauffman, and J. A. Smith, Review of Scientific Instruments **57** (8), 2179 (1986).
[8] S. H. Glenzer, B. J. MacGowan, P. Michel et al., Science **327** (5970), 1228.
[9] N. B. Meezan, L. J. Atherton, D. A. Callahan et al., (unpublished).
[10] P. Michel, S. H. Glenzer, L. Divol et al., (unpublished).
[11] J. C. Fernandez, S. R. Goldman, J. L. Kline et al., Physics of Plasmas **13** (5), 9 (2006).
[12] J. L. Kline, J. C. Fernandez, S. R. Goldman et al., J. Phys. IV **133**, 919 (2006).
[13] O. L. Landen, S. H. Glenzer, D. H. Froula et al., Eur. Phys. J. D **44** (2), 273 (2007).
[14] E. L. Dewald, S. H. Glenzer, O. L. Landen et al., Plasma Phys. Control. Fusion **47**, B405 (2005).
[15] E. L. Dewald, O. L. Landen, L. J. Suter et al., Physics of Plasmas **13** (5), 056315 (2006).
[16] E. L. Dewald, M. Rosen, S. H. Glenzer et al., Physics of Plasmas **15** (7), 072706 (2008).
[17] E. L. Dewald, L. J. Suter, O. L. Landen et al., Physical Review Letters **95** (21), 215004 (2005).
[18] R. E. Turner, O. L. Landen, P. Bell et al., Review of Scientific Instruments **70** (1), 656 (1999).
[19] G. B. Zimmerman and W. L. Kruer, Comments Plasma Phys. Control. Fusion **2** (2), 51 (1975).

Captions

Figure 1: Schematic layout of the scale-0.7 hohlraum target with directional locations of Dante, Static X-ray Imager (SXI), and backscatter diagnostics (Full Aperture Backscatter Station and Near Backscatter Imager).

Figure 2: Plot shows the experimental configuration of the targets including the four beam cones and dimensions of the scale 0.7 hohlraums. Included in the figure is a calculation of the specific energy stored in the coronal plasma for the flux-limited XSN (top) model with a flux limit of 0.05 and DCA (bottom) models with a flux limit of 0.15 at 2 ns in the laser pulse for 635 kJ.

Figure 3: a) input and output from a cable calibration from which the least squares filter is derived with (O) is every 50 point from the cable input, (– – –) is the output, and (—) is the result using filter to deconvolve the measured cable response for the input. The plot also shows the input signal recovery from application of the filter. b) an example of an in situ calibration of a cable using an ignition pulse shape.

Figure 4: Schematic setup of the calibration light box with a radiograph of a portion of the grid. A plot of the calibrations of the sieves is also shown.

Figure 5: Schematic layout of the setup for the sphere shot.

Figure 6: a) Plot of the (—) incident laser power and the (– – –) measured x-ray power versus time. b) Comparison of the (– – –) simulated radiated power and the (—) measured radiated power as a function of time.

Figure 7: Schematic diagram of the half hohlraum experimental layout with target dimensions.

Figure 8: Dante measurements of the flux for the (– – –) NIF early light half hohlraum experiments and the (—)current experiments using the same size target.

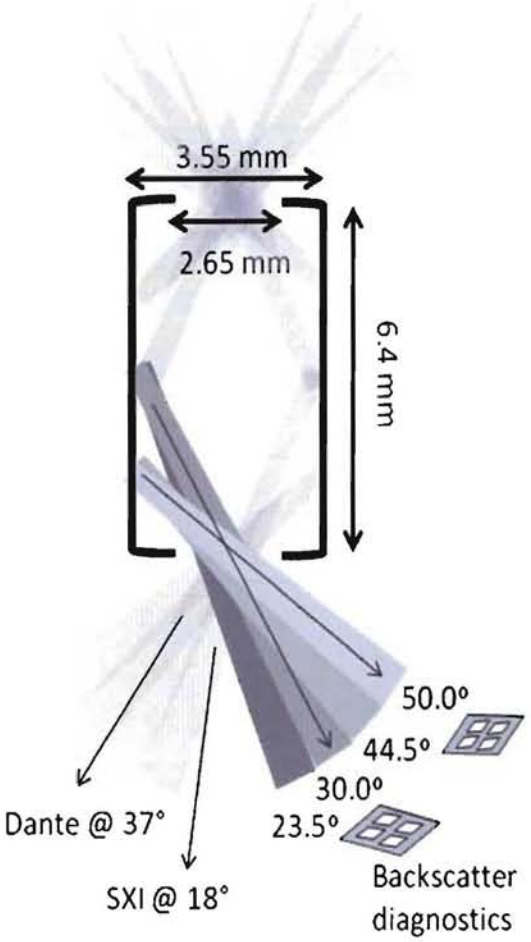

Kline figure 1

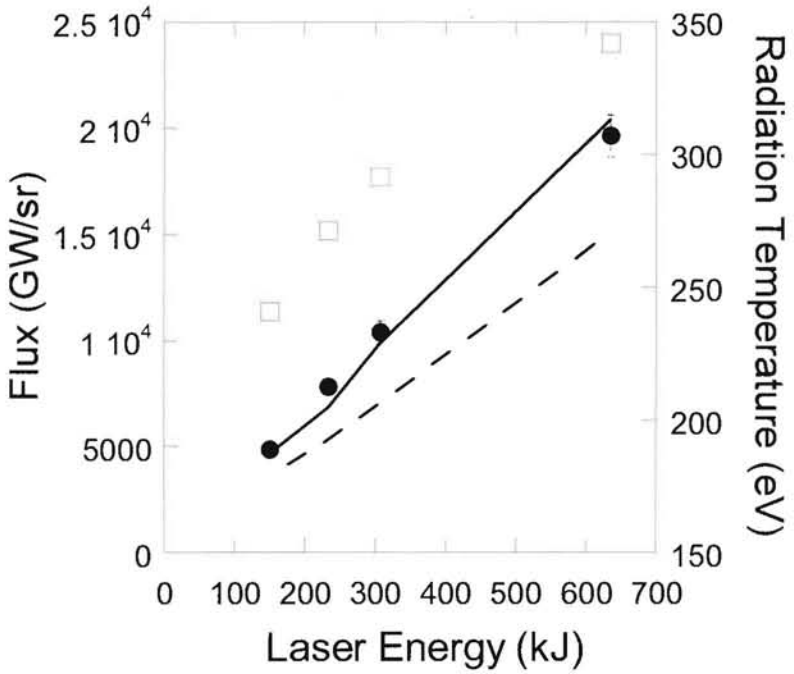

Kline figure 2

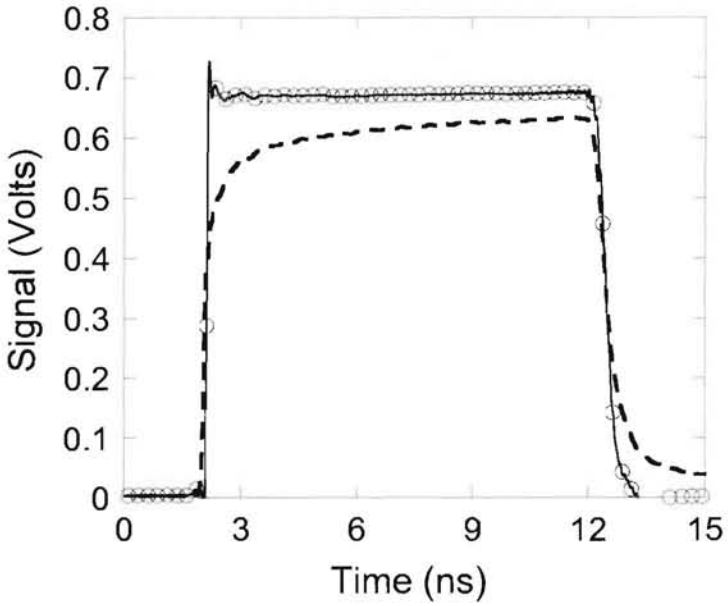

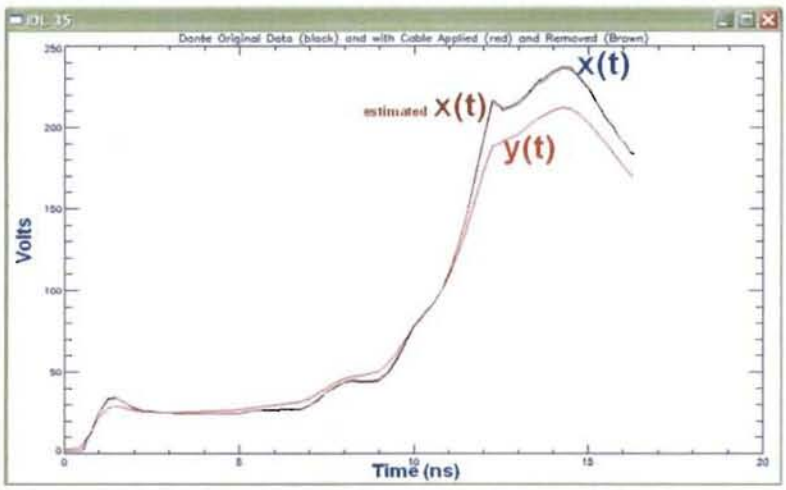

Kline figure 3

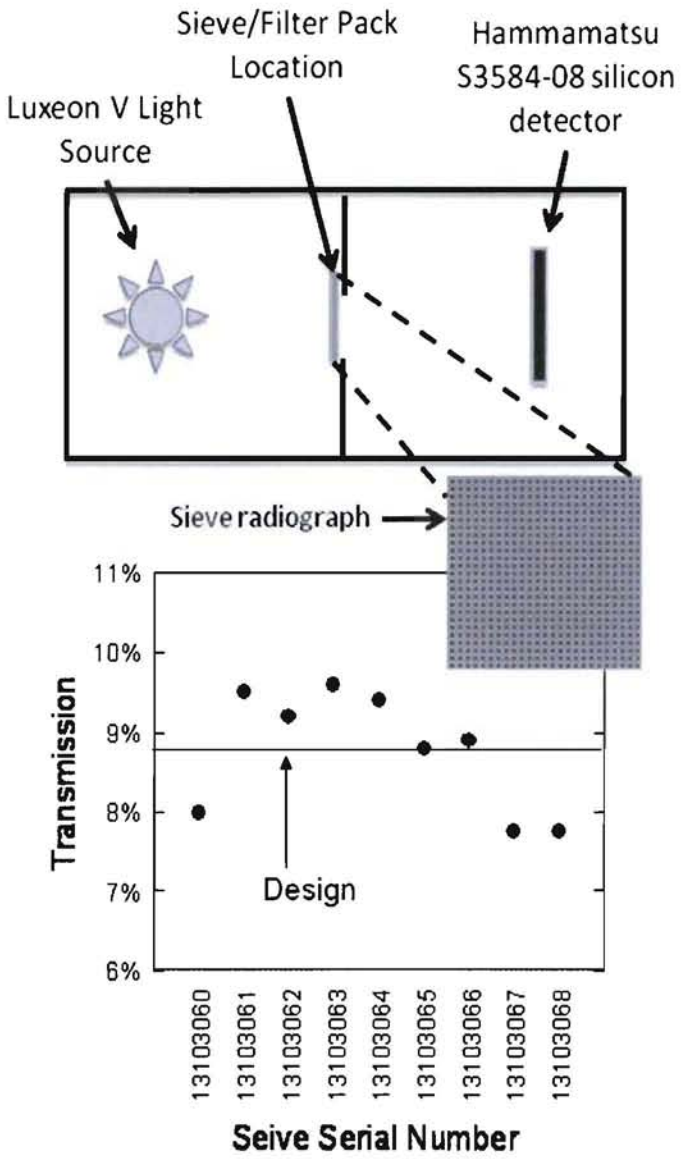

Kline figure 4

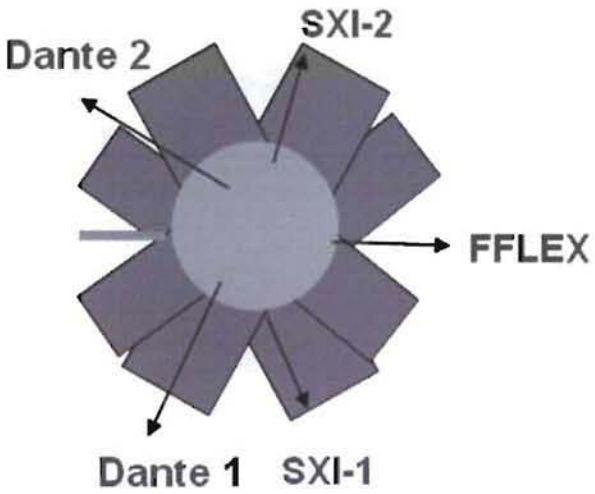

Kline figure 5

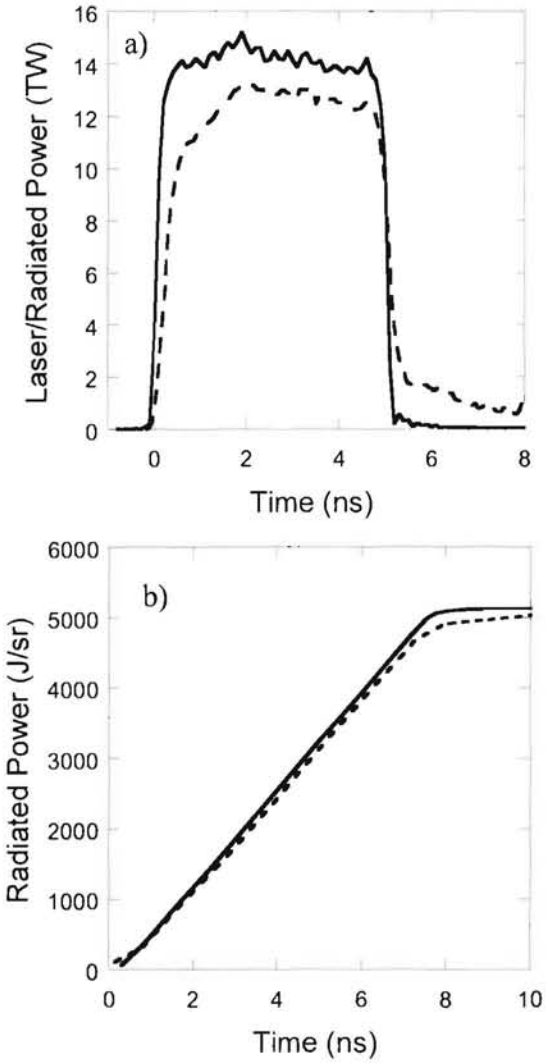

Kline figure 6

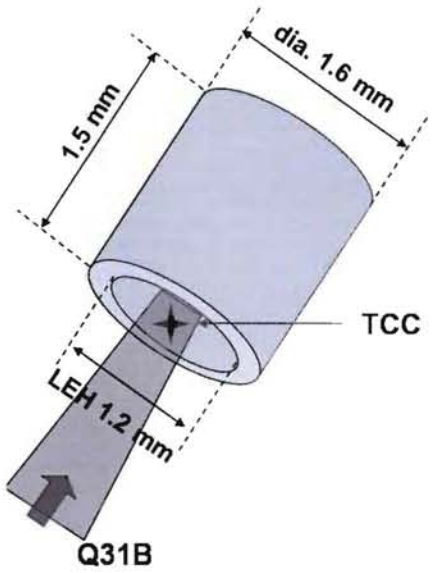

Kline figure 7

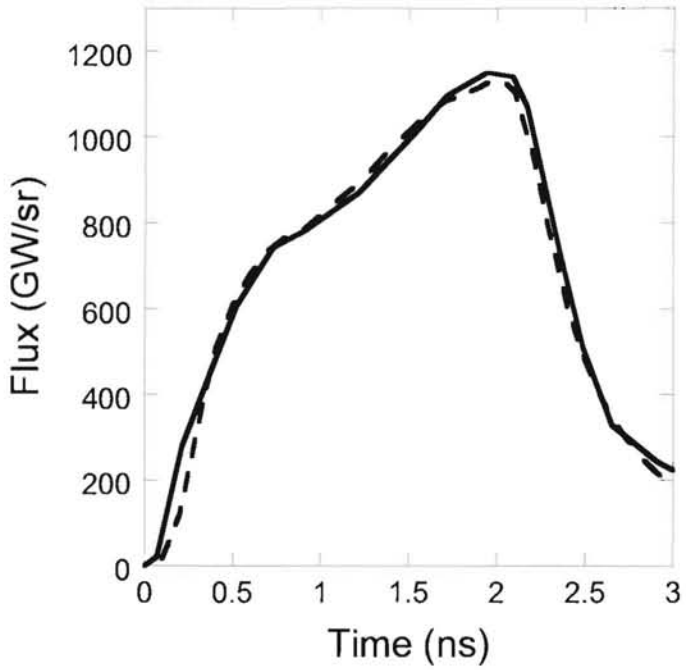
1200
1000
800
600
400
200
0
Flux (GW/sr)
0
0.5
1
1.5
2
2.5
3
Time (ns)